Proc. Natl. Acad. Sci. USA
Vol. 88, pp. 2768–2772, April 1991
Biochemistry

Analysis of affinity and structural selectivity in the binding of proteins to glycosaminoglycans: Development of a sensitive electrophoretic approach

MATTHIAS K. LEE* AND ARTHUR D. LANDER*†‡

*Department of Biology and †Department of Brain and Cognitive Sciences, Massachusetts Institute of Technology, Cambridge, MA 02139

Communicated by Phillip A. Sharp, December 13, 1990

ABSTRACT **Members of several families of cell surface and secreted proteins bind glycosaminoglycans (GAGs), the structurally heterogeneous polysaccharides found on proteoglycans. To understand the physiological significance of the interactions of proteins with GAGs, it is critical that relationships between GAG structure and binding be analyzed. It is particularly important that interactions depending on common structural features of GAGs (e.g., size, charge density, and disaccharide repeat unit) be distinguished from those mediated by specific sequences of carbohydrate modification. Gathering the information needed to make such distinctions has so far been difficult, however, partly because structurally homogeneous samples of GAGs are lacking but also because of technical difficulties associated with performing and interpreting assays of protein–GAG binding. We describe an electrophoretic method useful for both measuring affinity and evaluating structural selectivity in protein–GAG binding. Data are presented on the binding of the GAG heparin to the protease inhibitor antithrombin III, the acidic and basic fibroblast growth factors, and the extracellular matrix protein fibronectin. Results obtained with fibronectin are consistent with a model in which high-affinity binding ($K_d \approx 34$ nM) is mediated through the recognition of specific carbohydrate sequences.**

Proteins that bind glycosaminoglycans (GAGs) include many cell adhesion molecules, glycoproteins of the extracellular matrix, polypeptide growth factors, secreted proteases and antiproteases, and proteins involved in lipoprotein uptake (1, 2). In the tissue environments in which these proteins are found, GAGs are present as side chains of proteoglycans and exhibit diversity in length, disaccharide composition, and patterns of N- and O-sulfation.

For most GAG-binding proteins, the relationship between GAG structure and binding affinity is poorly understood. For some, all that is known is that a high concentration of salt is required to elute them from heparin-agarose columns; sometimes the relative abilities of GAGs of different classes (e.g., heparan sulfate, chondroitin sulfate, dermatan sulfate, keratan sulfate, etc.) to compete away such binding has also been measured (e.g., refs. 3 and 4). Those direct measurements of affinity that have been made have often required derivatization or immobilization of either protein or GAG (e.g., refs. 5–7); such measures may inhibit (e.g., by blocking sites of interaction) or artificially enhance (e.g., by favoring multivalent interactions) binding. Quantifying binding is also impeded by the fact that most GAG–protein K_d values are thought to be in the range of 5–500 nM, where the possibility of rapid dissociation kinetics argues against the use of many types of binding assays that involve separation and washing of bound complexes. In addition, measurements that have been made of GAG–protein affinity have usually measured the average affinity of a protein for the structurally heterogenous set of binding sites represented by any GAG sample. Selectivity of a protein for specific sequences of carbohydrate modification is, therefore, not readily appreciated, despite the fact that such selectivity exists and is, in at least one case, of considerable physiological importance (8).

Below, experiments are presented in which the principle of affinity electrophoresis (9) was exploited to analyze protein–GAG binding. The technique described is referred to as affinity coelectrophoresis (ACE) because both protein and GAG are permitted to migrate freely during electrophoresis (typically, in affinity electrophoresis, as in affinity chromatography, one ligand is physically immobilized). The method uses small amounts of material and can yield values of the affinity constant even when dissociation is rapid (e.g., when affinity is low). Experiments are presented in which ACE was used to identify and isolate a subpopulation of heparin molecules to which fibronectin binds selectively. Some of these data have been presented in abstract form (10, 11).

MATERIALS AND METHODS

Materials. Low-melting-point agarose (SeaPlaque) and GelBond were purchased from FMC, heparin (grade I, from porcine intestinal mucosa) was from Sigma, chondroitin sulfate (from shark cartilage) was from Fluka, bovine serum albumin (crystalline) was from ICN, and human plasma fibronectin (FN) was from New York Blood Center (New York). Basic fibroblast growth factor (bFGF) and acidic fibroblast growth factor (aFGF) were purified from bovine brain (12). Human antithrombin III (AT) was the generous gift of Robert Rosenberg (M.I.T.). β-Nerve growth factor was generously donated by Randall Pittman (University of Pennsylvania).

Heparin was substituted with fluoresceinamine to a level of 15.7 ng/μg (13) and radioiodinated to a specific activity of 110,000 cpm/ng (14). A portion of the ^{125}I-labeled fluoresceinamine-heparin (^{125}I-F-heparin) was fractionated by gel filtration [on Sephadex G-100 in 50 mM sodium 3-(*N*-morpholino)-2-hydroxypropanesulfonate) (Mopso), pH 7.0/125 mM sodium acetate] and the last 10.8% of the radioactive material to elute ($0.57 < K_{av} < 0.76$) was pooled as a low molecular weight (LMW) fraction. This fraction was estimated to contain heparin chains of $M_r \leq 6000$ (3, 15–18).

Electrophoretic Analysis of Binding. Low-melting-point agarose (1%) was prepared in either of two electrophoresis buffers: 50 mM sodium Mopso, pH 7.0/125 mM sodium acetate/0.5% 3-[(3-cholamidopropyl)dimethylammonio]-1-

The publication costs of this article were defrayed in part by page charge payment. This article must therefore be hereby marked "*advertisement*" in accordance with 18 U.S.C. §1734 solely to indicate this fact.

Abbreviations: ACE, affinity coelectrophoresis; aFGF and bFGF, acidic and basic fibroblast growth factor, respectively; AT, antithrombin III; CHAPS, 3-[(3-cholamidopropyl)dimethylammonio]-1-propanesulfonate; ^{125}I-F-heparin, ^{125}I-labeled fluoresceinamine-heparin; FN, fibronectin; GAG, glycosaminoglycan; LMW, low molecular weight; Mopso, 3-(*N*-morpholino)-2-hydroxypropanesulfonic acid.

‡To whom reprint requests should be addressed.

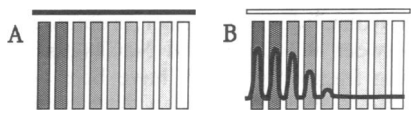

FIG. 1. Schematic representation of a gel before and after electrophoresis. Proteins are cast at various concentrations into nine rectangular zones within an agarose gel (*A*); the dark line at top represents a slot into which labeled GAG is introduced. During electrophoresis, GAGs migrate through the rectangular zones but are slowed by binding to proteins. This produces a series of peaks (*B*), from which an affinity constant may be derived (see text).

propanesulfonate (CHAPS) (buffer A) or 50 mM sodium Mopso, pH 7.0/125 mM NaCl/0.5% CHAPS (buffer B). A Teflon comb consisting of nine parallel bars, each 45 × 4 × 4 mm and held rigidly together with a spacing of 3 mm between bars, was placed onto GelBond film fitted to a Plexiglas casting tray (75 × 100 mm) with the long axis of the bars parallel to the long dimension of the tray. A Teflon strip (66 × 37 × 1 mm) was stood on edge with its long dimension parallel to the short dimension of the casting tray, at a distance of 4 mm from one edge of the Teflon comb. Tabs extending from the Teflon strip enabled it to be held upright by tape affixed to the casting tray. Typically, 19 ml of agarose were poured hot (>70°C) to achieve a cooled gel ≈4 mm thick. Removal of the comb and strip resulted in a gel containing nine 4 × 45 mm rectangular wells adjacent to a 66 × 1 mm slot (Fig. 1*A*).

Protein samples (typically 350 μl) were prepared in electrophoresis buffer at twice the desired concentrations. Samples were mixed with an equal volume of melted 2% (wt/vol) agarose at 37°C, pipeted into the appropriate rectangular wells, and allowed to gel. After submerging a protein-loaded gel in the electrophoresis chamber (Hoefer SuperSub) containing buffer minus CHAPS, ≈190 μl of ^{125}I-F-heparin [4 ng/ml in electrophoresis buffer containing 0.5% bromphenol blue and 6% (wt/vol) sucrose] was added to the 66 × 1 mm slot.

Typically, electrophoresis was performed at 60–70 V (2–2.4 V/cm) for 0.75–2 hr, with currents of ≈330 mA (in buffer A). Buffer was recirculated, and a flow of cold tap water through the coolant ports of the apparatus was used to maintain buffer temperature at 20–25°C. Endpoints were determined by the position of the bromphenol blue, which migrated about half as rapidly as heparin. Gels were air-dried and autoradiographed against preflashed film at −80°C. In some experiments, ^{125}I-F-heparin was recovered from gels by electroelution in 0.75 mM NaOAc/0.25 mM sodium Mopso, pH 7, concentrated 2-fold using a SpeedVac evaporator (Savant), and retested for binding using ACE.

RESULTS

Demonstration of Protein–GAG Binding. At neutral pH, the electrophoretic mobilities of most proteins are much lower than those of GAGs. Consequently, the binding of proteins to GAGs should, in most cases, retard GAG electrophoresis. To determine whether this effect could be exploited to quantify protein–GAG binding, a method was devised for electrophoresing labeled GAGs though zones containing multiple protein samples. Briefly, special combs were used to create agarose gels of the configuration shown in Fig. 1*A*. The long rectangles represent wells into which proteins in molten low-gelling-temperature agarose (at 37°C) could be introduced and allowed to gel. The dark line at the top of Fig. 1*A* indicates where samples of labeled GAGs were introduced. The position of the anode is at the bottom. Fig. 1*B* presents the expected experimental results when the nine wells contain a single GAG-binding protein at a series of concentrations decreasing from left to right: at sufficiently high protein concentrations, migration of the GAG front (thick black line) is retarded in a dose-dependent manner. The protein-free spaces between the wells facilitate measurement of the changes in mobility associated with each protein concentration.

Fig. 2*A* shows that the predicted pattern was indeed obtained when ^{125}I-F-heparin was electrophoresed at neutral pH and physiological ionic strength through zones containing a known heparin-binding protein, bFGF. In response to bFGF concentrations of up to 35 nM, heparin mobility was reduced up to 88%. The effect was specific, in that even much higher concentrations of nerve growth factor (a protein of similar size and isoelectric point to bFGF) had no effect on ^{125}I-F-heparin mobility (Fig. 2*B*).

An assumption made in predicting the simple pattern shown in Fig. 1*B* was that all heparin molecules behave more or less identically. The data in Fig. 2 *A* and *B* support this assumption. In contrast, experiments performed with a different heparin-binding protein, AT, illustrate the type of pattern that can result when heparin molecules do not behave identically (Fig. 2*C*). In this case, the migrating heparin front was split by AT into two distinct fronts, one of which was progressively slowed by AT concentrations ≥5 nM, whereas the other was shifted only slightly by AT at 1 μM. The same result was obtained with a size-selected LMW fraction of ^{125}I-F-heparin (Fig. 2*D*). A large excess of unlabeled heparin

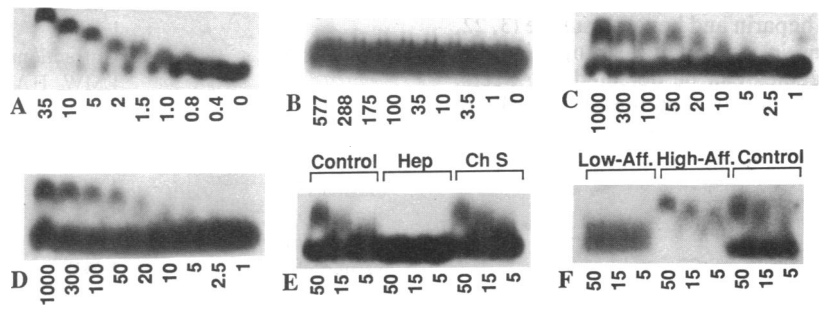

FIG. 2. (*A–D*) Autoradiographs of gels in which ^{125}I-F-heparin was electrophoresed through zones containing bFGF (*A*), β-nerve growth factor (*B*), and AT (*C* and *D*). Protein concentrations are in nM. (*B* and *D*) Size-selected LMW heparin was used. (*E*) Inhibition of binding of ^{125}I-F-heparin to AT by unlabeled heparin. In this experiment, a gel was cast with three sample slots, each opposite three of nine rectangular zones. Equal amounts of ^{125}I-F-heparin were introduced into each slot. In the central slot, unlabeled heparin (1 mg/ml) was mixed with the labeled sample; in the slot at right, unlabeled chondroitin sulfate (1 mg/ml) was added. Concentrations of AT are in nM. (*F*) Recovery and analysis of heparin with high and low affinity for AT. A set of three sample slots was prepared as in *E*. Into the slot at left was loaded material isolated from LMW ^{125}I-F-heparin that had previously migrated through AT-containing agarose without retardation (lanes Low-Aff.). Material that had been retarded by AT was isolated and loaded in the central slot (lanes High-Aff.). Control ^{125}I-F-heparin was loaded in the slot at right. Concentrations of AT are shown in nM.

readily blocked the effects of AT on heparin mobility, but an equal concentration of chondroitin sulfate did not (Fig. 2*E*).

These results fit with what is known about the properties of AT, one of the most studied GAG-binding proteins: AT binds a subset of heparin molecules, with subtleties of carbohydrate sequence, rather than heparin chain length, providing the basis for selectivity (19). To confirm that the two heparin fronts observed in ACE gels containing AT actually result from the fractionation of heparin into distinct species with different binding properties, a gel similar to the one shown in Fig. 2*D* was electrophoresed and pieces of agarose were cut out of locations where the two heparin fronts were well separated. The pieces were then melted, and their contents were retested for binding to AT. The results (Fig. 2*F*) confirm that separable fractions of heparin account for the pattern in Fig. 2*D*.

Measurement of Binding Affinity. In general, heparin's mobility in any protein-containing environment should be the average of the mobilities of protein-bound heparin and free heparin, weighted according to the fraction of time that heparin molecules spend in the bound and free states. To quantify protein-induced shifts in mobility, it is convenient to introduce a unitless number, the retardation coefficient R [$R = (M_o - M)/M_o$, where M_o is the mobility of free heparin and M is heparin's observed mobility through a protein-containing zone]. Provided that heparin and protein form a 1:1 complex, R at any protein concentration should be proportional to the amount of heparin bound. Moreover, if R_∞ is taken to represent the value of R seen at full saturation (i.e., at an arbitrarily high concentration of binding protein), then R/R_∞ should be equivalent to the fractional saturation. Accordingly, experimental values of R should vary with protein concentration according to the Scatchard equation; specifically, a plot of $R/[\text{protein}]_{\text{free}}$ vs. R should yield a straight line with a slope of $-1/K_d$ and a y intercept of R_∞/K_d. If the concentration of heparin is small compared to K_d, plotting $R/[\text{protein}]_{\text{total}}$ vs. R should yield the same plot.

Two such plots are shown in Fig. 3. The data for bFGF binding to LMW heparin (Fig. 2*A*) fit a line implying a K_d of 2 nM. For AT binding to LMW heparin, values of R obtained from Fig. 2*D* also fit a line, implying a K_d of 16 nM (Fig. 3*B*). Straight lines also fit the data obtained for the binding of unfractionated heparin to bFGF and AT, and for the binding of heparin to aFGF and serum albumin (data not shown). These findings are summarized in Table 1. Results with two buffer systems that differed in their major anion (chloride vs. acetate) did not differ significantly.

Characterization of Heparin Binding to FN. FN is a major glycoprotein of the extracellular matrix and a component of plasma (20, 21). FN binds heparin and heparan sulfate (3, 22, 23), whereupon alterations in its structural properties and ability to bind other molecules can be detected (e.g., refs. 24–26). Recent evidence indicates that the attachment of epithelial cells and fibroblasts to FN is mediated, in part, by cell surface heparan sulfate (27, 28).

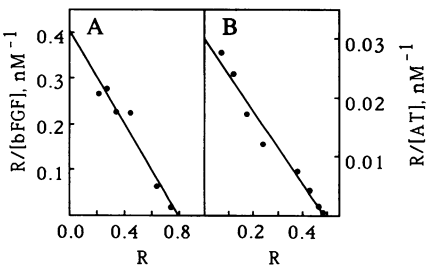

FIG. 3. Graphic analysis of binding of bFGF to LMW heparin (*A*) and binding of AT to the high-affinity fraction of LMW heparin (*B*). The lines drawn imply K_d values of 2 nM for bFGF and 16 nM for AT.

Plasma FN, a disulfide-linked dimer, is eluted from heparin-Sepharose between 0.3 and 0.5 M NaCl (29). Two distinct heparin-binding fragments of FN have been identified and mapped. Yamada *et al.* (3) used a filter-binding assay to measure the binding of [^{3}H]heparin to FN and obtained a biphasic Scatchard plot, suggestive of two component affinities (K_d values of 4.2 nM and 110 nM), but were unable to determine whether their data reflected differences in the affinity of heparin for two distinct sites on FN or the presence of subspecies of heparin that bind FN with different affinities. In addition, values of K_d were derived assuming that heparin molecules contain only one binding site for FN. This assumption may not be valid, especially given that particularly long heparin chains (average M_r, 12,000) were used in that study (3).

Analysis of the heparin–FN interaction by ACE is shown in Fig. 4*A*. At high FN concentrations, LMW ^{125}I-F-heparin was observed to shift to a single very low mobility, implying that essentially all heparin molecules bind FN. At somewhat lower FN concentrations, however, the labeled material migrated not as a discrete band but as a diffuse smear. It seemed likely that this smear represented the fractionation of individual heparin molecules according to differences in affinity for FN.

To test this possibility, LMW ^{125}I-F-heparin was electrophoresed through a single zone of 125 nM FN. The gel was then cut transversely into segments, and fractions were pooled representing the leading 26% of the ^{125}I-F-heparin (pool 1, "weakly retarded heparin") and the trailing 26% (pool 2, "strongly retarded heparin"). The samples were heated to 100°C for 10 min (to denature FN) and labeled heparin was recovered by electroelution. The resulting material was retested for binding to FN. As shown in Fig. 4 *B* and *C*, the ACE patterns for pools 1 and 2 were distinctly different from each other and considerably less diffuse than those of the starting material.

Graphical analysis of the patterns in Fig. 4 *B* and *C* is shown in Fig. 5. The data from pool 1 yield a linear plot, suggesting a K_d of 640 nM. Pool 2 yields an apparently discontinuous plot—two line segments with similar slopes (implying K_d values of 32 and 36 nM). Examination of Fig. 4*C* indicates how the result for pool 2 arises: with increasing FN concentration, heparin's mobility decreases, levels off at $R \approx 0.5$,

Table 1. Measurement of protein affinities for heparin and LMW heparin

Protein	Heparin	K_d, nM
bFGF	Unfractionated	2.2
	LMW	2.0
	LMW	3.1*
AT	Unfractionated, HA	11
	LMW, HA	16
	LMW, HA	12*
	Unfractionated, LA†	≈6000
aFGF	LMW	91
Plasma FN	LMW, HA‡	34
	LMW, LA‡	640
Nerve growth factor	LMW	>600§
Serum albumin	LMW	4300

Measurements were made in buffer A except for those indicated by an asterisk, which were made in buffer B. HA and LA refer to strongly retarded (high affinity) and weakly retarded (low affinity) fractions, respectively, as isolated from ACE gels (see text). As described in the *Discussion*, correct values of K_d for bFGF may be lower by as much as 0.8 nM.

†Estimated from data in Fig. 2*C* and the assumption that R_∞ for low-affinity heparin will be the same as that observed for high-affinity heparin.

‡From the experiment described in Figs. 4 and 5.

§Highest concentration tested.

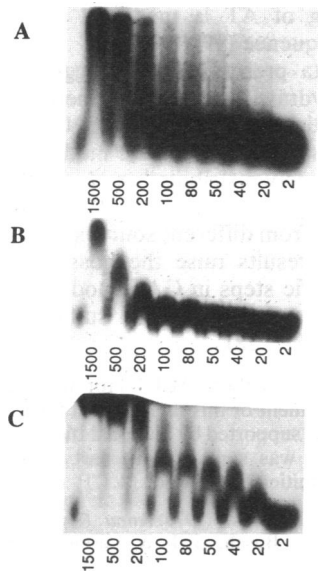

FIG. 4. Analysis of heparin–FN binding. (*A*) Electrophoresis of ^{125}I-F-heparin through zones containing FN (concentrations in nM, based on a molecular weight of 440,000). In contrast to the examples in Fig. 1, the migrating heparin front becomes broadly smeared at protein concentrations between 50 and 500 nM. (*B* and *C*) After electrophoresis of ^{125}I-F-heparin in the presence of 125 nM FN, the 26% of labeled material that was retarded least (pool 1) and the 26% of labeled material that was retarded most (pool 2) were recovered by electroelution and retested for binding to FN. The patterns produced by pool 1 (*B*) and pool 2 (*C*) are distinctly different.

and then shifts again, leveling off at $R \approx 0.8$. This behavior is most easily explained by the known tendency of FN to self-aggregate when concentrated (see ref. 30). Thus, the first shift (to $R \approx 0.5$) may represent saturation of heparin by single FN molecules, whereas the second shift (to $R \approx 0.8$) reflects aggregation of FN molecules into oligomers (which, being larger, more strongly retard heparin's mobility). In support of this view, studies in which trace amounts of ^{125}I-labeled FN were electrophoresed in the presence of unlabeled FN showed that the mobility of FN in 2% agarose undergoes a concentration-dependent decrease (consistent with aggregation) in the expected range (10–200 nM) (unpublished observations).

Thus the data in Figs. 4 and 5 indicate that LMW heparin is heterogeneous and that classes of heparin molecules that differ by as much as 20-fold in affinity for FN can be isolated. To test whether this difference in affinity depends on heparin size (chain length), pools 1 and 2 were compared by gel

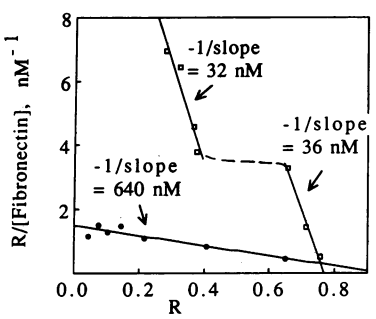

FIG. 5. Graphic analysis of data in Fig. 4 *B* and *C*. Weakly retarded heparin (●) yields a linear plot implying a K_d value of 640 nM. Strongly retarded heparin (□) yields a discontinuous plot with two line segments that imply K_d values of 32 nM and 36 nM. The discontinuity apparently reflects oligomerization of FN at high concentrations (see text).

filtration on Sephadex G-75 in 10 mM Mopso, pH 7.0/125 mM sodium acetate/4 M urea. The size distributions of molecules in pools 1 and 2 were largely overlapping, with those of pool 1 being slightly smaller ($K_{av} = 0.250$) and those in pool 2 slightly larger ($K_{av} = 0.162$) than the LMW heparin from which both pools were derived ($K_{av} = 0.235$) (data not shown). To assess whether the molecules in pools 1 and 2 differed greatly in charge density (a reflection of the degree of sulfation), their electrophoretic mobilities in 1% agarose (containing no binding proteins) were compared. The mobilities obtained for the two pools were identical: $5.6 \pm 0.03 \times 10^{-8}$ m^2/V·s for pool 1 and $5.6 \pm 0.05 \times 10^{-8}$ m^2/V·s for pool 2 (in buffer A at 25°C).

DISCUSSION

We report here the development of an affinity-electrophoretic technique, ACE, for studying GAG–protein interactions. Binding is measured at physiological pH and ionic strength and under conditions in which interacting molecules are freely mobile. ACE can in principle be used to measure binding between any two macromolecules, provided that the complex they form has an electrophoretic mobility different from that of at least one of its components. In practice, this difference should be large enough that distances migrated by bound and free ligand are distinguishable within reasonable time. In some of the experiments described above, it was possible to achieve sufficient separations with electrophoresis of the GAG front through only 20 mm of gel; in no experiment was electrophoresis through >50 mm necessary. These distances required short electrophoresis times at modest field strengths (e.g., 2.4 V/cm for 1–2 hr). Also, because electrophoresis was carried out in a gel of small width and height, little material was required. For example, to measure binding of heparin to AT in Fig. 2*E*, only 400 pmol of protein and 75 fmol of GAG were used. Considering that ACE can measure affinities when dissociation rates are fast and that other techniques for doing so [e.g., equilibrium gel filtration (31, 32)] can require large amounts of material, the sensitivity of ACE seems particularly good.

Accurate determination of affinity constants using ACE requires that the following conditions be met. (*i*) The radiolabeling of one component should not affect binding. (*ii*) The physical properties of the gel should not affect binding. (*iii*) The kinetics of association and dissociation should be rapid compared to the time of electrophoresis. In the experiments reported here, heparin was substituted with <1 fluoresceinamine per molecule and radioiodinated (14); the possibility that labeling interfered with binding is argued against by ACE experiments on the binding of intact proteoglycans (labeled by protein radioiodination) to FN and the binding of heparan sulfate (metabolically labeled) to AT, which have yielded results similar to those reported here (ref. 11; T. Kojima, G. Marchildon, and R. Rosenberg, personal communication). Also, electrophoresis was performed using a highly porous matrix (1% agarose) to minimize effects of sieving on molecular interactions, and electrophoresis times were long (1–2 hr) compared with likely kinetic constants.

As shown in Figs. 3 and 5, it is convenient to analyze ACE data by plotting $R/[\text{protein}]_{total}$ vs. R and to obtain an apparent value of K_d from the slope. Strict validity of this procedure has the following three requirements.

(*i*) **Concentration of GAG Is Much Less Than the K_d.** Use of the total, rather than the free, concentration of protein in the Scatchard equation is convenient, because it does not require the concentration of labeled heparin to be known accurately. This substitution is valid as long as the total concentration of heparin is sufficiently low. Otherwise, deviations from linearity at low values of R will occur, leading to a possible overestimation of K_d (by an amount no greater than the heparin concentration itself). The results in Table 1 were

obtained using heparin at 4 ng/ml, which for LMW heparin chains (estimated M_r, 5000–6000) is equivalent to 0.7–0.8 nM (for unfractionated heparin, the molar concentration would be lower). At this heparin concentration, the K_d values in Table 1 should be reasonably accurate with one exception: For the binding of bFGF to LMW heparin, the measured K_d of 2.0–3.1 nM should probably be revised to 1.2–2.4 nM.

***(ii)* Mobilities of GAG–Protein Complexes Are Independent of Protein Concentration.** The assertion that the retardation coefficient R is proportional to the fractional saturation of GAG by protein assumes that the GAG–protein complex has a single fixed mobility. In some cases this may not be true, as results obtained with FN illustrate. Because of protein–protein interactions, mobility of the heparin–FN complex is lower at high FN concentrations than at low FN concentrations, giving rise to a nonlinear Scatchard plot (Fig. 5).

***(iii)* GAGs Are Not Multivalent.** The binding of a second (or third, etc.) protein molecule to a GAG is not likely to produce as large a change in mobility as the binding of the first. Accordingly, if GAGs are multivalent, ACE data will tend to emphasize the behavior of the first site to saturate. If multiple sites of equivalent affinity are present, the Scatchard plots obtained may, for statistical reasons, be nonlinear and possess slopes that lead to an underestimation of the intrinsic K_d of the binding sites (by a factor not exceeding the number of binding sites). A more detailed treatment of the effects of multivalency and protein–protein interactions on ACE patterns will be presented elsewhere (unpublished results).

In this study, measurements were made of the affinity of several proteins for heparin. Where prior information on affinity is available, it agrees reasonably well with the results presented here. For example, affinity chromatographic studies of heparin binding to AT indicate that two populations of heparin exist, one with high affinity and one with low affinity, and that the latter species is more abundant in commercial preparations of heparin (8, 33); the data in Fig. 2 *E* and *F* imply both of these statements. The K_d values reported in Table 1 for the binding of heparin to AT are within or close to the range of values that have been published by others, namely, 12.5–100 nM for the high-affinity fraction of heparin and 20–100 μM for the low-affinity fraction (5, 8, 16). Methodological differences or differences in the ionic composition of buffers may account for the ranges of values.

For bFGF, the values in Table 1 agree reasonably well with affinities reported for the binding of this growth factor to cell surface heparan sulfate, namely, 0.5 nM (34) and 2 nM (35), especially if the values in Table 1 are corrected as described above. The affinity of 91 nM obtained with aFGF is consistent with the fact that the binding of this growth factor to heparin-agarose is apparently weaker than that of bFGF (36).

For FN binding to heparin, ACE analysis uncovered evidence of selective binding of FN to subpopulations of heparin molecules. Although classes exhibiting two distinct K_d values were identified, they were derived from the 52% of heparin molecules that were either most strongly or most weakly retarded; therefore, it is possible that molecules with intermediate affinities were also present. When heparin subpopulations binding strongly and weakly to FN were compared, no difference in overall charge density was detected. Strongly binding heparin molecules were, however, slightly larger on average than weakly binding ones. These are precisely the properties expected if high-affinity binding to fibronectin is mediated by one or more specific rare carbohydrate sequences. A slightly larger size for high-affinity molecules is predicted on statistical grounds, as rare sequences are expected to be most common on long chains (15). Indeed, the same phenomenon has been observed with AT: fractionation of heparin populations by their affinity for AT produces a high-affinity fraction with an average size slightly larger than the low-affinity fraction (15, 16) despite the fact that the binding of AT is mediated by a specific short carbohydrate sequence (19).

If, as the data presented here suggest, FN recognizes specific carbohydrate sequences on heparin, it will be important to investigate the binding of FN to heparan sulfates, which bear the same carbohydrate modifications as heparin but which are widely distributed *in vivo*. Interestingly, large differences have been reported in the degree to which heparan sulfates from different sources bind FN (e.g., refs. 3 and 37). These results raise the possibility that cells, by controlling specific steps in GAG modification, could modulate their ability to use heparan sulfate as a cell-surface receptor for FN (27, 28).

We thank Dr. R. Rosenberg (M.I.T.) for many helpful discussions during the development of this method and for the generous gift of AT. This work was supported by National Institutes of Health Grant NS26862. M.K.L. was supported in part by the Undergraduate Research Opportunities Program of M.I.T.

1. Lindahl, U. & Hook, M. (1978) *Annu. Rev. Biochem.* **47,** 385–417.
2. Jackson, R. L., Busch, S. J. & Cardin, A. D. (1991) *Physiol. Rev.* **71,** 481–539.
3. Yamada, K. M., Kennedy, D. W., Kimata, K. & Pratt, R. M. (1980) *J. Biol. Chem.* **255,** 6055–6063.
4. Del Rosso, M., Cappalletti, R., Viti, M., Vannucchi, S. & Chiarugi, V. (1981) *Biochem. J.* **199,** 699–704.
5. Rosenberg, R. D., Oosta, G. M., Jordan, R. E. & Gardner, W. T. (1980) *Biochem. Biophys. Res. Commun.* **96,** 1200–1208.
6. Jordan, R. E., Oosta, G. M., Gardner, W. T. & Rosenberg, R. D. (1980) *J. Biol. Chem.* **255,** 10073–10080.
7. Skubitz, A. P. N., McCarthy, J. B., Charonis, A. S. & Furcht, L. T. (1988) *J. Biol. Chem.* **263,** 4861–4868.
8. Bjork, I. & Lindahl, U. (1982) *Mol. Cell. Biochem.* **48,** 161–182.
9. Horejsi, V. (1981) *Anal. Biochem.* **112,** 1–8.
10. Lee, M. K. & Lander, A. D. (1989) *J. Cell Biol.* **109,** 109 (abstr.).
11. Herndon, M. E., Lee, M. K. & Lander, A. D. (1990) *J. Cell Biol.* **111,** 267 (abstr.).
12. Lobb, R. R. & Fett, J. W. (1984) *Biochemistry* **23,** 6295–6299.
13. Glabe, C. G., Harty, P. K. & Rosen, S. D. (1983) *Anal. Biochem.* **130,** 287–294.
14. Smith, J. W. & Knauer, D. J. (1987) *Anal. Biochem.* **160,** 105–114.
15. Laurent, T. C., Tengblad, A., Thunberg, L., Hook, M. & Lindahl, U. (1978) *Biochem. J.* **175,** 691–701.
16. Jordan, R., Beeler, D. & Rosenberg, R. (1979) *J. Biol. Chem.* **254,** 2902–2913.
17. Rosenberg, R. D., Jordan, R. E., Favreau, L. V. & Lam, L. H. (1979) *Biochem. Biophys. Res. Commun.* **86,** 1319–1324.
18. Danielsson, A. & Bjork, I. (1981) *Biochem. J.* **193,** 427–433.
19. Lindahl, U., Thunbereg, L., Backstrom, G., Riesenfeld, J., Norling, K. & Bjork, I. (1984) *J. Biol. Chem.* **259,** 12368–12376.
20. Hynes, R. O. (1985) *Annu. Rev. Cell Biol.* **25,** 295–305.
21. Ruoslahti, E. (1988) *Annu. Rev. Biochem.* **57,** 375–413.
22. Ruoslahti, E. & Engvall, E. (1980) *Biochim. Biophys. Acta* **631,** 350–358.
23. Stamatoglou, S. C. & Keller, J. M. (1982) *Biochim. Biophys. Acta* **719,** 90–97.
24. Welsh, E. J., Frangou, S. A., Morris, E. R., Rees, D. A. & Chavin, S. I. (1983) *Biopolymers* **22,** 821–831.
25. Osterlund, E., Eronen, I., Osterlund, K. & Vuento, M. (1985) *Biochemistry* **24,** 2661–2667.
26. Johansson, S. & Hook, M. (1980) *Biochem. J.* **187,** 521–524.
27. Gill, P. J., Silbert, C. K. & Silbert, J. E. (1986) *Biochemistry* **25,** 405–410.
28. Saunders, S. & Bernfield, M. (1988) *J. Cell Biol.* **106,** 423–430.
29. Yamada, K. M. (1983) *Annu. Rev. Biochem.* **52,** 761–799.
30. Homandberg, G. A. (1987) *Biopolymers* **26,** 2087–2098.
31. Hummel, J. P. & Dryer, W. J. (1962) *Biochim. Biophys. Acta* **63,** 530–532.
32. Horwitz, A., Duggan, K., Greggs, R., Decker, C. & Buck, C. (1985) *J. Cell Biol.* **101,** 2134–2144.
33. Lam, L. H., Silbert, J. E. & Rosenberg, R. D. (1976) *Biochem. Biophys. Res. Commun.* **69,** 570–577.
34. Walicke, P. A., Feige, J.-J. & Baird, A. (1989) *J. Biol. Chem.* **264,** 4120–4126.
35. Moscatelli, D. (1987) *J. Cell Physiol.* **131,** 123–130.
36. Lobb, R. R., Harber, J. W. & Fett, J. W. (1986) *Anal. Biochem.* **154,** 1–14.
37. Laterra, J., Ansbacher, R. & Culp, L. A. (1980) *Proc. Natl. Acad. Sci. USA* **77,** 6662–6666.